AR-NE7A/2016G004

X-Ray Fluorescence Computed Tomography Imaging of Gold Nanoparticles

Tenta Sasaya [1], Seung-Jun Seo [2], Naoki Sunaguchi [3], Tsutomu Zeniya [4], Kazuyuki Hyodo [5], Jong-Ki Kim [2], and Tetsuya Yuasa [1,*]

[1] Yamagata University, [2] Catholic University of Daegu, [3] Nagoya University, [4] Hirosaki University, [5] KEK

Gold nanoparticles (GNPs) have attracted attention in nanomedicine as novel contrast agents for cancer imaging. They can selectively accumulate within a tumor and remain there for longer durations compared to conventional iodinate contrast agents. Their specificity can be increased through the active targeting achieved by conjugation with antibodies or peptides directed against tumors. In addition to the active specific tumor targeting and slower clearance, they offer a noteworthy advantage that they have been shown to enhance the local dose deposition for x-ray radiotherapy. For cancer diagnosis, planning, and treatment, it is very important to develop a tool to identify, quantify, and locate GNPs distributed in a biological object. In this study, we proposed a tomographic imaging method to visualize the distribution of NPs with a spatial resolution of sub-millimeters using x-ray fluorescence emitted from the NPs, and constructed a prototype x-ray fluorescence computed tomography (XFCT) system using synchrotron radiation as an incident beam. This report describes the imaging principle of XFCT from the viewpoint of measurement science, and shows some preliminarily experimental results for demonstrating the efficacy.

We constructed the XFCT imaging system at the bending-magnet beamline AR-NE7A in KEK. A PILATUS 100K manufactured by DECTRIS Ltd. was used. In this study, we paid attention to the L-shell fluorescence of Au (L_α: 9.71 keV, L_β: 11.4 keV) because the quantum efficiency at energies around 10 keV is approximately 90%, and the photoelectric cross section at incident energies around the L-edge of Au is approximately 20 times higher than that around the K-edge. We used the monochromator to select an incident energy of 25 keV, which was the minimum energy set in the beamline, so that the incident energy was as close as possible to the L-edge energy of Au within the allowable range to produce more L-shell fluorescence photons. The flux was approximately 5.0×10^8 photons/mm^2/s in front of the object. The cross section of the incident beam was collimated to 35 mm (horizontal) × 5 mm (vertical) by the slit. The distance between the rotational axis and the collimator plane was 27.5 mm, and the distance between the collimator plane and the detector surface was 30.0 mm. The rotational stage and the detector were controlled by a PC. We imaged a physical phantom consisted of a 10-mm-diameter PMMA cylinder with three 3-mm-diameter channels filled with GNPs solution of different concentrations (1.0, 2.0, and 4.0 Au mg/ml), as shown in Fig. 1.

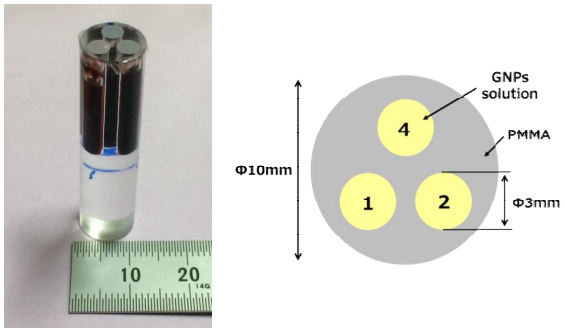

Fig. 1 Physical phantom: The photograph (left) and the cross section (right).

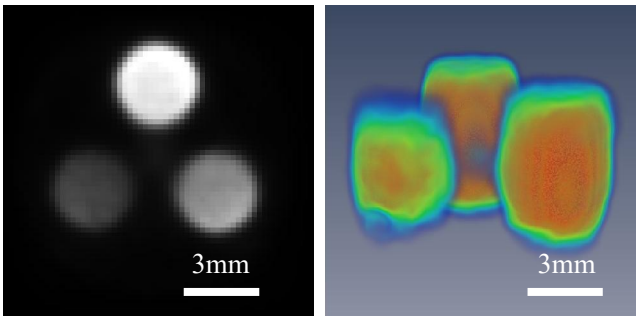

Fig. 2 Reconstructed image: The cross sectional image (left), the 3-D volume rendering image (right).

Fig. 2 shows the cross sections at the central level of the 3-D reconstructed image of the phantom and the image in the volume rendering (VR) representation. While the Au regions are distorted in the VR image, the distortion mainly was caused by the inhomogeneous distribution of intensity in the incident beam. Analysis of the image revealed that the spatial resolution was about 0.3 mm, and the imaging method enabled highly quantifiable measurement. We obtained a satisfactory 3-D reconstructed image. We are planning *ex-vivo* imaging of rat's brain and heart in near future.

References

1. T. Yuasa *et al.*, *IEEE Trans. Nucl. Sci.* **44**, 54 (1997).
2. T. Sasaya *et al.*, *Sci. Rep.* **7**, 22143 (2017).
3. T. Sasaya *et al.*, *Sci. Rep.* **7**, 5742 (2017).
4. T. Sasaya *et al.*, *Nucl. Inst. Meth. A* **886**, 71 (2018).

*yuasa@yz.yamagata-u.ac.jp